Biological Control 145 (2020) 104261

Contents lists available at ScienceDirect

Biological Control

journal homepage: www.elsevier.com/locate/ybcon

A new species of *Trichoderma* and gliotoxin role: A new observation in enhancing biocontrol potential of *T. virens* against *Phytophthora capsici* on chili pepper

Ali Athafah Tomah[a,b,c], Iman Sabah Abd Alamer[a,b,d], Bin Li[a,b], Jing-Ze Zhang[a,b,*]

[a] Institute of Biotechnology, Zhejiang University, 310058 Hangzhou, China
[b] State Key Laboratory of Rice Biology and Ministry of Agriculture Key Lab of Molecular Biology of Crop Pathogens and Insects, China
[c] Plant Protection, College of Agriculture, University of Misan, AL-amarah 62001, Iraq
[d] Plant Protection, Agriculture Directorate, Maysan Province, AL-amarah 62001, Iraq

ARTICLE INFO

Keywords:
Taxonomy
Trichoderma dorothopsis
Mass spectrometric analysis
Antagonistic activity
Mechanism of action

ABSTRACT

Phytophthora capsici is a phytopathogen causing a destructive pepper blight. To control this disease, 77 isolates of *Trichoderma* spp. were isolated from rhizosphere soil and 15 isolates showed high antagonistic activity. Based on the analysis of the rDNA internal transcribed spacers (*ITS*), translation elongation factor 1-α (*TEF1*) and RNA polymerase II subunit B (*RPB2*) gene sequence data and morphological traits, the isolates were identified as *T. brevicompactum*, *T. atroviride*, *T. afroharzianum*, *T. koningiopsis*, *T. citrinoviride*, *T. asperellum*, *T. harzianum*, *T. virens* and a new species. A new species was described as *T. dorothopsis*. The *in vitro* antagonistic assay and analysis of metabolite fractions indicate that the *T. virens* HZA14 could cause colony collapse and degradation of *P. capsici*. A high activity compound was identified as gliotoxin by spectrometric analysis. The biocontrol tests demonstrated that the *T. virens* HZA14 delayed the occurrence of chili pepper blight and significantly reduced the disease incidence and severity by 62.64% and 64.20%, respectively. Hence isolate HZA14 could be considered for developing potential biocontrol agent for management of *P. capsici* in pepper.

1. Introduction

Phytophthora disease caused by *Phytophthora capsici* is the most destructive disease on pepper plants grown in greenhouses and fields (Granke et al., 2015). The disease usually occurs in the underground parts of a plant, leading to root and crown rot of pepper. During a serious disease epidemic, pathogen dispersal causes aerial blight of leaves, fruit and stems (Callaghan et al., 2016). The white mycelia with zoosporangia often produce on the water-soaked lesions under the humid conditions (Foster and Hausbeck, 2010). Irreversible pepper blight generally develops quickly, resulting in the plant death. Pepper blight is one of important diseases on chilli and bell pepper in Zhejiang province and it occurs severely each year (Jiang et al., 2016a).

For management of the diseases, agricultural and chemical methods, such as crop rotation, resistant varieties and the use of fungicides are widely applied. However, among these strategies, the crop rotation is not widely chosen due to the limitation of agricultural areas and long-term survival of pathogen oospores that are resistant to desiccation, cold temperatures, and other extreme environmental conditions in soil (Quesada-Ocampo et al., 2009; Roberts et al., 2008). In relation to genetic resistance, the availability of resistant varieties is not common (Foster and Hausbeck, 2010). Moreover, highly resistant pepper cultivars showed susceptibility or moderate resistance when the plants were inoculated with *P. capsici* (Dunn and Smart, 2015).

Management of *P. capsici* relies on use of common-use fungicides metalaxyl and mefenoxam, resulting in the development of fungicide resistance in the *P. capsici* (Barchenger et al., 2018; Parra and Ristaino, 2001) and environmental or human health problems (Hausbeck and Lamour, 2004). Biological control is a promising and sustainable approach for the effective management of phytopathogenic fungi. *Trichoderma* species, such as *T. asperellum* (Jiang et al., 2016a), *T. harzianum* (Ezziyyani et al., 2007; Sid Ahmed et al., 1999), *T. koningiopsis* (Ramírez-Delgado et al., 2018), have been shown to be particularly effective in management of *P. capsici*. However, the introduction of new strains of *Trichoderma* in the soils has had limited success, probability due to the poor competition and adaptation ability, and the complexity

* Corresponding author at: Yuhangtang Road 866, Nongshenghuan Building C703, Institute of Biotechnology, Zijingang campus, Zhejiang University, Hangzhou 310058, China.
E-mail address: jzzhang@zju.edu.cn (J.-Z. Zhang).

https://doi.org/10.1016/j.biocontrol.2020.104261
Received 26 July 2019; Received in revised form 2 March 2020; Accepted 20 March 2020
Available online 21 March 2020

of the soil environment (Hyakumachi et al., 2013; Savazzini et al., 2009).

Trichoderma spp. possess many antagonistic mechanisms against pathogens of crops, such as lytic enzymes, mycoparasitism, competition for nutrients and space and so on, for their successful colonization (Harman, 2006; Mukherjee et al., 2012). For example, Jiang et al. (2016a) revealed that the hyphae of *T. asperellum* isolate CGMCC 6422 could penetrate the hyphae and oospores of *P. capsici* by mycoparasitism, leading to the degradation of hyphal cells. Mycoparasitism involves cell wall degrading enzymes (CWDEs), which allows mycoparasitic fungi to bore holes into other fungi and extract nutrients for their own growth (Cao et al., 2009). Also, *Trichoderma* strains produce antibiotics or low-molecular-weight compounds, which inhibit the growth of plant pathogens such as 6-pentyl-pyrone (Jeleń et al., 2014), viridiofungin (El-Hasan et al., 2009), gliotoxin (Roberts and Lumsden, 1990), etc. However, the mechanisms by which the *Trichoderma* spp. suppresses different types of pathogens are different among species and strains. In particular, the ability to produce the antibiotics vary between isolates of the same species as well as between isolates of different species (Dennis and Webster, 1971). So for different pathogens, screening the isolates of *Trichoderma* spp. with highest antagonistic activity and characterizing their antagonistic mechanisms are becoming more and more common for their application as biocontrol agents (Vinale et al., 2008).

In this study, therefore, we screened native isolates of *Trichoderma* spp. with antagonistic activity against *P. capsici*, with the specific aims to (i) identify these isolates by morphological characteristics and molecular sequences (*ITS*, *TEF1*, and *RPB2*) and (ii) evaluate the underlying mechanisms such the production of antagonistic compounds. This will provide the potential isolates for developing of the effective biocontrol agents against pepper blight by *P. capsici* that will work in the region.

2. Materials and methods

2.1. Pathogen isolate

The *Phytophthora capsici* HZ07 was a highly aggressive isolate and it was isolated previously from the diseased roots of *Capsicum annuum* cv. Hangxian No. 3 and identified as the A2 mating types (Jiang et al., 2016a). It was deposited at 11–12 °C in the Culture Collection of Biotechnology Institute, Zhejiang University, Zhejiang Province, China.

2.2. Isolation of Trichoderma spp.

Forty soil samples were collected from the rhizosphere of bell or chili pepper plants in the heavily infested fields by *P. capsici* from eight different farms near to Hangzhou city, China. All soil samples were stored at 4 °C in the laboratory. Serial dilutions were made with each soil sample. For this, 1 g of soil was added into 9 ml of sterile distilled water, the suspension was shaken and then a series of dilutions were carried out. An aliquot of 1 ml of each diluted soil suspension was uniformly spreaded on the surface of a *Trichoderma* selective medium (TSM: $MgSO_4{\cdot}7H_2O$ 0.2 g; K_2HPO_4 0.9 g; KC1 0.15 g; NH_4NO_3 1.0 g; glucose 3.0 g; chloramphenicol 0.25 g; rose-bengal 0.15 g; agar 20 g with 1 L water) (Elad et al., 1981) and the plates were incubated at 27 ± 1 °C for four days. Colonies grewing on TSM were transferred to the potato dextrose agar (PDA) for their single spore isolation. The single spore isolates were stored at 4 °C for use in this study.

2.3. Screening of antagonistic isolates

The dual culture technique was used to screen the isolates with highest antagonistic activity against *P. capsici* HZ07. For this, a disc (5-mm diameter) from the margin of a three-day-old colony of a *Trichoderma* isolate was put on one side on a PDA plate (9-cm diameter), with another 5 mm of five days old mycelia of *P. capsici* was placed on the opposite side. Each treatment was replicated three times. The plates were incubated at 25 ± 1 °C. Degree of antagonism was assessed for each isolates on a scale of classes 1–5 (1 = *Trichoderma* sp. grew completely on the pathogen and covered the whole surface of the culture medium; 2 = *Trichoderma* sp. grew on at least two-thirds of the culture medium; 3 = each *Trichoderma* sp. and the pathogen colonized nearly half of the culture medium and no organism dominated the other; 4 = at least two-thirds of the culture medium was colonized by the pathogen and the pathogen resisted encroachment of the antagonist; 5 = the pathogen grew completely on the *Trichoderma* sp. and colonized the whole surface of the culture medium) (Zhang et al., 2015).

2.4. Molecular identification

The fungal isolates were cultured in a 250 ml flask containing 100 ml potato dextrose broth (PDB), shaken at 150 rpm at 27 ± 1 °C for four days. The mycelia were filtered and grounded to a fine powder in liquid nitrogen. Genomic DNA was extracted using a protocol described by Zhang and Li (2009). The obtained genomic DNA was resuspended in 50 μL TE buffer and stored at −20 °C. Three DNA fragments were amplified in an automated thermal cycler (Eppendorf AG, Germany). The primer pairs ITS5 and ITS4 were used for amplification of rDNA *ITS* regions (Jiang et al., 2016b), the primers EF1-728F (5′-CATCGAGAAGTTCGAGAAGG-3′) (Carbone and Kohn, 1999), and TEF1LLErevR (5′-AACTTGCAGGCAATGTG G-3′) (Samuels et al., 2002) for the translation elongation factor 1 α (*TEF1*) gene and primers RPB2-5F (5′-GAYGAYMGWGATCAYTTYGG-3′) and RPB2-7cR (5′-CCCATRG-CTTGYTTRCCCAT-3′) for the RNA polymerase II subunit B (*RPB2*) gene (Jiang et al., 2016a). The purified PCR products were submitted to the Sangon Biotech Company Limited (Shanghai, China) for sequencing in both directions.

2.5. Phylogenetic analysis

The sequences were edited by BioEdit 7.1.3.0 (Hall, 1999) and analyzed by the nucleotide BLAST search in the GenBank database. They were deposited in GenBank and reference sequences were downloaded from GenBank (Supplementary Table 1). Phylogenetic tree was constructed by using the three-locus combined *ITS*, *TEF1*, and *RPB2* dataset with 60 in group taxa and two outgroup taxa (*Nectria berolinensis* and *N. eustromatica*) (Supplementary Table 1). The sequences of each region or genes were aligned with MAFFT v7.273 (Katoh and Standley, 2013) and edited by the BioEdit. The resulting sequences were analyzed by Gblocks 0.91b for eliminating the ambiguously aligned positions and divergent regions prior to phylogenetic analyses (Katoh and Standley, 2013). The model of evolution for each alignment was estimated by using jModel Test 2.1.7 (Darriba et al., 2012) and the model chosen according to the Akaike information criterion. The best TrNef + I + G model was selected for *TEF1* and CTR + I + G for *RPB2* and TrNef + I + G for *ITS*.

The molecular phylogenies of *Trichoderma* spp. were analyzed by Maximum likelihood (ML) and Bayesian inference (BI). ML analyses were implemented with RaxmlGUI v. 1.5 (Silvestro and Michalak, 2012). ML bootstrap (ML- BS) analysis of each ML tree completed with a fast 1000 bootstrap frequency with the same parameter settings using the GTR + I + G model of the nucleotide substitution. The 80% values were showed on a tree for significantly supported nodes. BI analyses are conducted with MrBayes v. 3.2.6 (Ronquist et al., 2012). The MCMC (Markov-chain Monte-Carlo) used to seek in four chains; these branches have been run on 10 million generations with 100 tree samples every generation. The remaining trees merged into one tree with 50% majority rule consensus tree. BI posterior probability (BI-PP) values equal or above 0.95 were found to be significant.

2.6. Morphological observation

The isolates were cultured on PDA, cornmeal dextrose agar (cornmeal agar 20 g, dextrose 20 g, agar 20 g with 1 L distilled water) and synthetic low nutrient agar (KH_2PO_4 1.0 g, KNO_3 1.0 g, $MgSO_4{\cdot}7H_2O$ 0.5 g, KCl 0.5 g, glucose 0.2 g, sucrose 0.2 g, agar 15.0 g with 1 L water) and incubated at 20–25 °C under an alternating cycle of 12 h light and 12 h darkness (Jaklitsch, 2009). The fungal asexual structures such as conidiophores, phialides, conidia and chlamydospores were observed and measured using a Zeiss Axiophot 2 microscopy with Axiocam CCD camera and Axiovision digital imaging software (AxioVision Software Release 3.1., v.3–2002; Carl Zeiss Vision Imaging Systems). The closely related species on phylogenetic tree were morphologically compared by taxonomic characteristics.

2.7. Detection of activity metabolites

To evaluate active metabolites produced by 15 isolates of *Trichoderma* against *P. capsici*, a mycelia-disc (5 mm) obtained from the isolate cultured on PDA was transferred into a 250 ml flask containing 100 ml PDB and the flasks were incubated in a ZWY-211B rotary shaker for 14 days. After filtering mycelium from the culture liquid with cheesecloth, the used culture medium was centrifuged and 50% (V/V) and 20% culture liquids were prepared by dilution and then sterilized by filtration through millipore membrane with 0.22 μm pore size. One ml of each culture liquid was added into a 9-cm-diameter plate containing 10 ml molten PDA, and then a mycelia-disc (0.5 cm) of five days old *P. capsici* was placed into the centre of a plate. Plates with PDA but without culture liquid were used as the controls. Each treatment was replicated five times. The plates were kept at 25 °C, and the diameter of the colonies was measured when the diameter of control colonies reached the plate edge. Inhibition percentage of mycelial growth was calculated using the formula: IP (%) = [(C − T)/C)] × 100, where IP is the inhibition percentage, C is the control hyphal growth diameter, T is the hyphal growth diameter in the culture liquid-treated plates.

2.8. Purification and identification of active fractions

Based on the results of the previous experiments, the highest active fractions produced by the *Trichoderma* isolates were purified and their chemical structures were identified. The isolates screened were inoculated into a flask containing PDB and incubated in a rotary shaker for 14 days, as descibed above. Two litres of culture liquid were obtained and the metabolites were extracted using ethyl acetate. The solvent was evaporated under reduced pressure. The residue was purified by silica gel column chromatography (particle size 200–300 mesh) and different fractions were purified by preparative silica gel TLC (GF_{254}). A small amount of each fraction was dissolved in DMSO (dimethyl sulfoxide) for bioactive determination. Aliquots of 1 ml of each fraction (100 μg/ml) were added into 10 ml of molten PDA in each plate then, a mycelia-disc (5 mm) of *P. capsici* was placed onto the plate centre. The active fractions were determined by observing of pathogen growth onto the plates (absence or presence) after incubation at 25 °C for four days. To identify chemical structures, the active fractions were purified further with a Waters 600 HPLC instrument fitted with a Shimpack Prep ODS column (20 × 250 mm). The eluent was monitored with a Waters 2487 Dual λ absorbance detector at 254 nm. Good semi-preparative separation of the active fraction peaks was obtained with a flow rate 6 μL/minutes by isocratic elution with the mixture of methanol and distilled water (1:1, V/V). The mass spectrum of active fraction was analyzed with a VG Autospec-3000 mass spectrometer (VG, Manchester, UK) and API QSTAR Pulsar 1 (Applied Bio-systems, Foster City, USA). For further bioactive determination, the purified compound was dissolved in DMSO and different mother solutions were obtained. For this, they were mixed with a molten V8 medium and seeded onto plates at final concentration of 0.5, 1.0, 5.0, 10.0 and 15.0 μg/ml. Mycelial discs (5 mm) of *P. capsici* were placed into the centre of V8 media plate. Each treatment was replicated five times. The plates were kept at 25 °C for four days and colony diameters were measured when the diameter of control colonies reached the plate edge. Inhibition percentage of mycelial growth was calculated, as described above.

2.9. Effect of antagonistic isolates against chili pepper blight

Based on previous experiment results, the *Trichoderma* isolates were used for *in vitro* tests of biocontrol against chili pepper blight. Seeds of chili pepper (*Capsicum annuum* L. cv Jizua) were sterilized with 2% sodium hypochlorite solution, placed into the surfaces of the wet sterilized filter papers that were in a plate, and the plates were incubated at 25 °C for 5–6 days. The germinated seeds were sowed into the pots (11 × 11 × 11 cm) containing the soil mixture (peat: vermiculite: farmyard soil in a 2:1:1 ratio) and incubated at 28–30 °C and relative humidity level of 80–90%. *Trichoderma* isolates were cultured in the flasks containing wheat grains autoclaved and incubated at 25 °C with a 12 h photoperiod for 15 days for fungal conidial production. One hundred of mL of sterile water was poured into each conical flask and vortexed vigorously to dislodge the spores. Spore suspensions were collected in a container. Spores were counted using a hemocytometer. For soil inoculation, the 10-ml conidial suspension (about 1×10^7 spores/mL) was applied around the root zone of each seedling with six to eight leaf stage. One week after inoculation, each pot was inoculated with 5 ml of zoospores suspension (about 2×10^3 zoospores/mL) of *P. capsici* (Bosland and Lindsey, 1991). For preparation of pathogenic inocula, the five mycelia discs of *P. capsici* were put into a plate with 10 ml of sterile distilled water and incubated at 25 °C under light condition for three days for zoosporangial production. The zoospores suspension was prepared by incubating plates at 4 °C for 30 min for zoospore release, filtration with cheesecloth and quantification with a hemocytometer, as described by Ristaino (1990). Seedlings inoculated only with zoospores suspension were used as control. Each treatment (with 25 plants) was repeated three times. The plants were observed daily and disease incidence (DI %) and disease severity (DS %) were recorded after 15 days from inoculation. Disease severity was assessed using a scale of classes 0–4, where 0 = no symptoms, 1 = wilting of the plant, without a stem lesion, 2 = wilting and stem lesion without girdling, 3 = girdled plant stem, 4 = dead plant (Ristaino, 1990).

All statistical analyses were done using SPSS software version 16 (SPSS, Chicago, IL, USA) and the level of significance for the LSD test was set at $P < 0.05$.

3. Results

3.1. Isolation and screening of antagonistic isolates

A total of 77 isolates of *Trichoderma* spp. were obtained from the rhizosphere soil. Among them, 19.5% (n = 15) of *Trichoderma* isolates showed the highest antagonistic activity with antagonism class 1, while 80.5% of the isolates had antagonism classes for 2–5. The 15 isolates with antagonism class 1 (Fig. 1) were chosen as the antagonistic candidates and they were designated as HZA1-HZA15. A distinct interaction zone of hypha disappearance of *P. capsici* HZ07 in the interaction between *P. capsici* and *Trichoderma* sp. isolate HZA14 was observed (Fig. 1). For confirming this phenomenon, the repeated test showed that colonization of the HZA14 was able to lead to a clear interaction zone of hypha disappearance of *P. capsici* HZ07 (Fig. 2). Microscopic observation showed that near margin of a interaction zone of *P. capsici* hyphal disappearance, the hyphae of *P. capsici* were penetrated and encircled by hyphae of *T. virens*, leading to its hyphal degradation (Fig. 3B and 3C). Especially, it was found that the part of a hypha of *P. capsici* was killed but it's another part was normal yet (Fig. 3A). In addition, complete disintegration of *P. capsici* hyphae was common in the

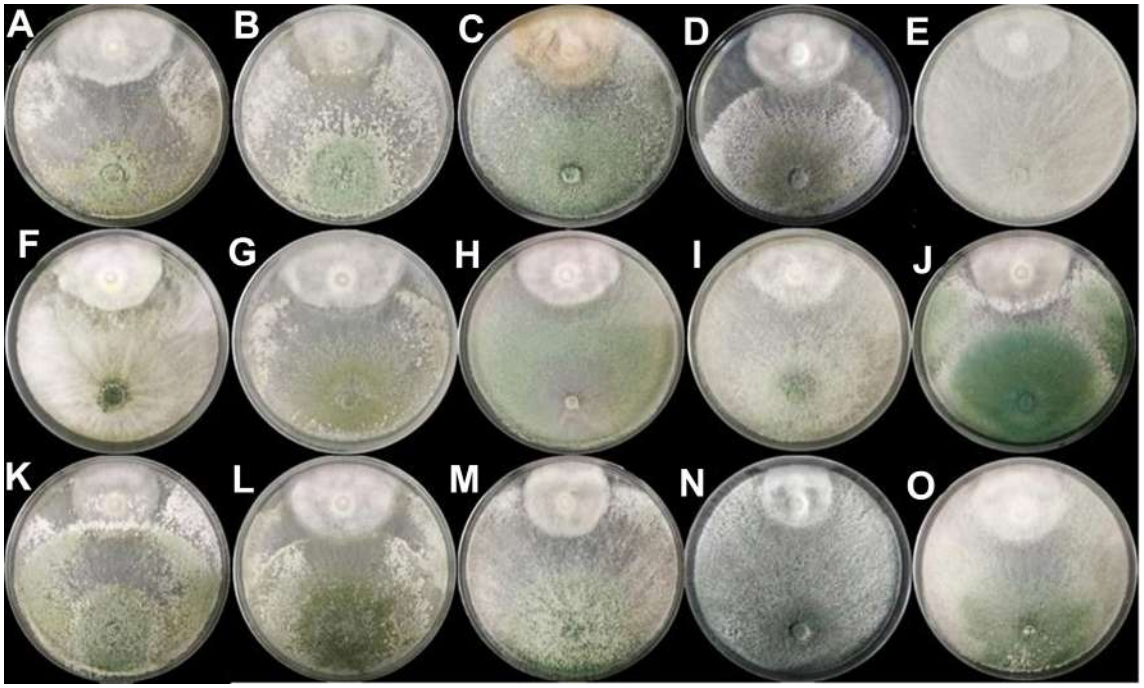

Fig. 1. Antagonistic effect of 15 isolates (bottom) with antagonism class for 1 on the hyphae of *P. capsici* (upper parts) on PDA five days after inoculation. A. HZA1. B. HZA2. C. HZA3. D. HZA4. E. HZA5. F. HZA6. G. HZA7. H. HZA8. I. HZA9. J. HZA10. K. HZA11. L. HZA12. M. HZA13. N. HZA14. O. HZA15.

Fig. 2. The isolate HZA14 causing the interaction zone (*) of hyphal disappearance of *P. capsici*.

interaction zone (Fig. 3D).

3.2. Sequence and phylogenetic analysis

The genomic DNA of 15 isolates amplified by primer pairs ITS6 F/ITS4 R, EF1-728F/TEF1LLErevR and RPB2-5F/RPB2-7cR produced the fragments of approximately 630 bp (*ITS*), 1300 bp (*TEF1* region) and 1077 bp (*RPB2*), respectively. Sequences of each Trichoderma isolate were aligned, edited, analyzed and deposited in the GenBank database (Supplementary Table 1).

To delineate species boundaries, phylogenetic analysis was carried out by using the three-locus combined *ITS*, *TEF1* and *RPB2* dataset. After removing the ambiguously aligned regions, the alignments were

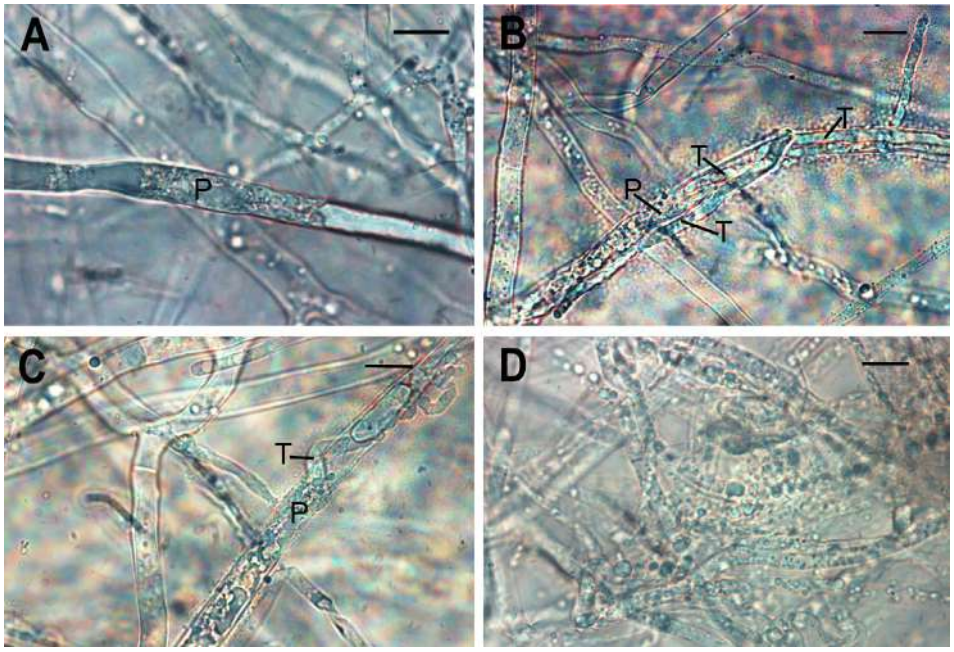

Fig. 3. Antagonism of *T. virens* HZA14 against *P. capsici* HZ07 in a collapsed interaction region after hyphae of *T. virens* overgrowing the colony of *P. capsici*. A. A partially killed hypha of *P. capsici* (P). B. A hypha of *T. virens* (T) around a disintegrated hypha of *P. capsici* (P). C. A hypha of *T. virens* (T) encircling a disintegrated hypha of *P. capsici*. D. Lots of disintegrated hypha of *P. capsici*. Scale bars = 10 μm.

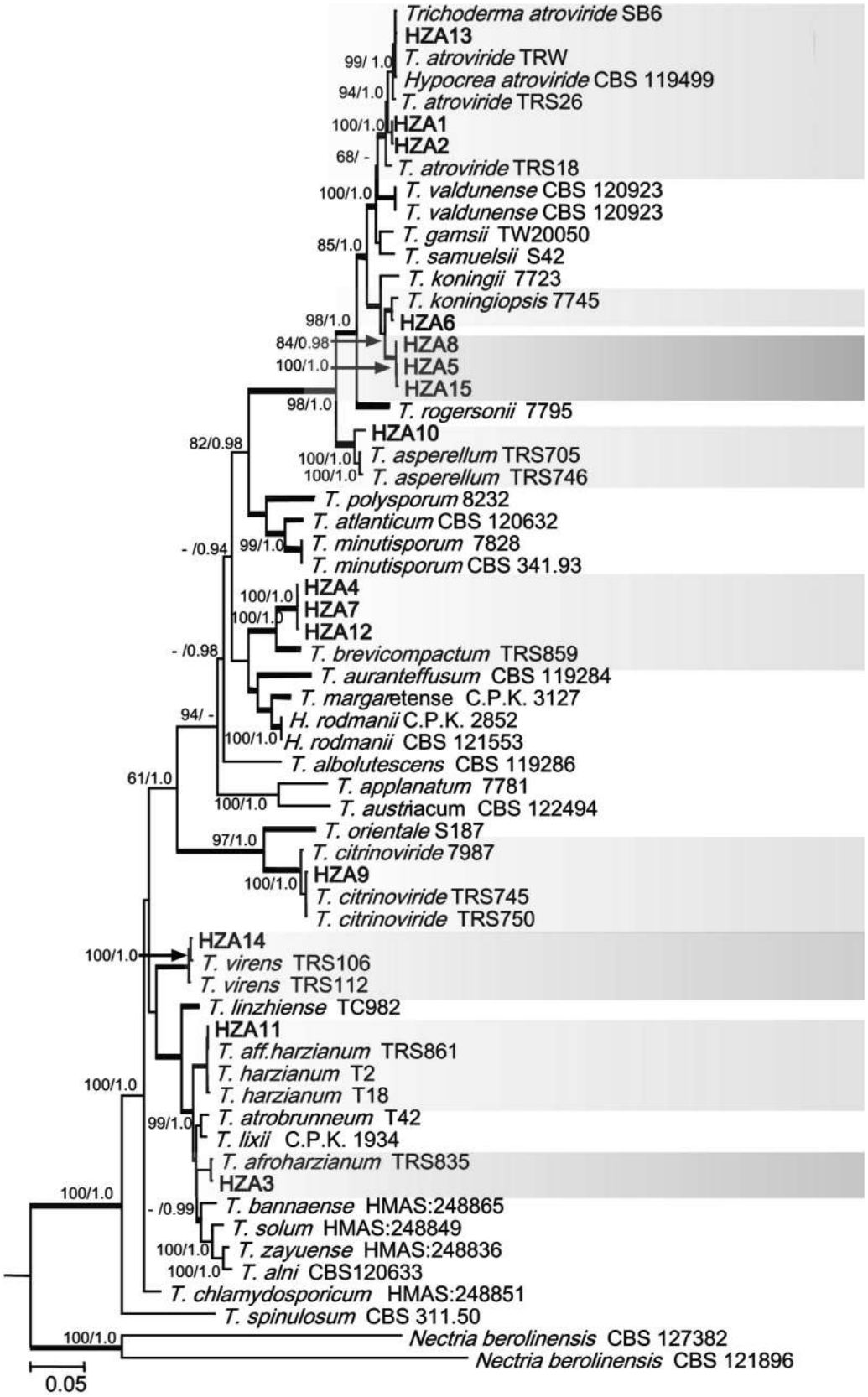

Fig. 4. Maximum likelihood (ML) tree generated from the combined *ITS*, *TEF1* and *RPB2* sequences of 62 taxa of *Trichoderma*. The tree is rooted with *Nectria berolinensis* and *N. euchromatica.* Clades with 100% ML bootstrap branch support and 1.00 Bayesian posterior probabilities (BPP) are indicated by thick black lines. Clades with > 80% ML-BS (left) and 0.95 BPP (right) are indicated by the corresponding support values. Dashes indicate support values lower than 80% ML-BS and 0.95 BPP. Species isolated from the rhizosphere of pepper plants are shown in bold.

2034 characters, of which 609 were phylogenetically informative. The parsimony informative characters were 243 in *TEF1* alignment, 277 in *RPB2* and 89 in *ITS*, respectively. The phylogenetic tree showed that all studied isolates were separated into different clades (Fig. 4). The topology of the best scoring ML tree analysis was congruent with the BI tree for the concatenated three-locus dataset. The relationship of most all reference isolates could be clearly distinguished on the level of species. The isolates HZA13, HZA1 and HZA2 clustered with *T. atroviride* SB6, *T. atroviride* TRW, *H. atroviride* CBS 119499 and *T. atroviride* TRS 26 as a clade with high ML-BS (100%) and high BI-PP (1.00) support. The isolates HZA8, HZA5 and HZA15 clustered as a distinct clade with high ML-BS (100%) and high BI-PP (1.00) support, forming a sister clade with tested isolate HZA6 and *T. koningiopsis* 7745 to the well-supported clade with higher ML-BS (84%) and higher BI-PP (0.98) support. The phylogenetic analysis indicated that isolates HZA8, HZA5 and HZA15 have a close relationship, and *T. koningiopsis* being more closely related to the HZA6. Similarly, HZA4, HZA7 and HZA12 clustered as a distinct clade with high ML-BS (100%) and high BI-PP (1.00) support, forming a sister clade with *T. brevicompactum* TRS859 with high ML-BS (100%) and high BI-PP (1.00) support. In addition, HZA10, HZA9, HZA14, HZA11 and HZA3 clustered with *T. asperellum* TRS705 and TRS746, *T. citrinoviride* TRS745 and TRS750, *T. virens* TRS106 and TRS112, *T. aff. harzianum* TRS861, *T. harzianum* T5 and *T. harzianum* T18, and *T. afroharzianum* TRS835 as a distinct clade with high ML-BS (100%) and high BI-PP (1.00) support, respectively.

3.3. Taxonomy

3.3.1. ***Trichoderma dorothopsis*** *A.A. Tomah & J.Z. Zhang, sp. nov.*

MycoBank: MB 831,879 Fig. 5

Holotype: CHINA, ZHEJIANG PROVINCE: Shaoxin, from Soil, 30°18′3"N, 120°51′3"E, 5.7 M, 2 Jun. 2017, A.A. Tomah and J.Z. Zhang (HOLOTYPE dry culture HMAS 248251 and ex-type living culture CGMCC3.19672 = HZA5).

Etymology: "dorothopsis" in reference to the similarity to *T. dorotheae* with phialides tending to proliferate percurrently to form new phialides.

Description: The optimum temperature for growth on PDA and SNA is 27–30 °C. Colonies grown on PDA producing conidia within 96 h, with abundant aerial mycelium without the concentric rings (Fig. 5A); on CMD abundant yellowish conidia in the aerial mycelium forming differentiated concentric rings (Fig. 5B); on SNA conidia beginning to form small pustules in a ring around the original inoculum in marked concentric rings (Fig. 5C). No diffusing pigment or distinctive odour detected on any medium. On SNA, conidial masses green to deep green. Conidial production nearly continuous with a tendency to form highly compact to cottony, 1–2 mm diam pustules (Fig. 5D − 5E). Often long, entirely fertile branches visible in the pustules (Fig. 5F). Conidiophores comprising a recognizable main axis; fertile branches arising along the length of the main axis, more or less paired with longer or shorter internodes (Fig. 5G). The longer branches near the base and short branches or solitary phialides arising near the tip (Fig. 5H); branches rebranching or producing directly phialides (Fig. 5I); sometimes several phialides arising from the same point and crowded (Fig. 5K). Phialides, (9.76-) 9.69–11.43 (-11.92) × (2.54-) 3.06–3.89 (-4.36) µm, narrowly lageniform, straight, only slightly swollen in the middle. In some cases, phialides tending to proliferate percurrently to form new phialides (Fig. 5I − 5J). Conidia, (3.19-) 3.34–3.91 (-4.18) (avr. 3.63) × (2.86-) 3.07 × 3.48 (-3.56) (avr. 3.28) µm, globose to subglobose, occasionally ellipsoidal, smooth (Fig. 5l). Chlamydospores, abundant, terminal to intercalary, globose to subglobose (Fig. 5M).

Specimens examined: CHINA, ZHEJIANG PROVINCE: Hangzhou, from Soil, 30°3′36″N, 120°49′22″E, 5.7 M, 2 Jun. 2017, J.Z. Zhang (living culture CGMCC3.19673 = HZA8, CGMCC3.19674 = HZA15). The living cultures HZA5, HZA15, and HZA8 were deposited in the Culture Collection of Biotechnology Institute, Zhejiang University, Zhejiang Province, China.

Comments: *Trichoderma dorothopsis* is characterized by main axis branched conidiophores, lush aerial mycelium production on CMD, narrowly lageniform phialides tending to proliferate percurrently to form new phialides, smooth, globose to subglobose conidia but with yellow coloration on CMD. It has a closest phylogenetic relationship with *T. koningiopsis* and *T. koningii* and clusters with *T. koningiopsis* (Fig. 4), which is morphologically distinct. *T. dorothopsis* producing lush aerial mycelium on CMD, being different from *T. koningii* and *T. koningiopsis* with very little aerial mycelium (Samuels et al., 2006). It has narrowly lageniform phialides but lacks intercalary phialides comparing with *T. koningiopsis*. Unlike *T. koningii* with oblong conidia and *T. koningiopsis* with ellipsoidal conidia, *T. dorothopsis* has globose to subglobose conidia. In addition, *T. dorothopsis* produces phialides tending to proliferate percurrently to form new phialides, being similar to *T. dorotheae* (Samuels et al., 2006).

3.3.1.1. Identification of other species. The isolates HZA4, HZA7 and HZA12 grown on CMD or SNA, conidiophores pyramidally verticillately branched in the Pachybasium-type patterns (Bissett, 1991). Phialides mostly broadly ampulliform with a short slender neck. Conidia, 2.6–3.1 × 2.1–2.9 µm, subglobose to short ellipsoidal. Based on morphological characteristics, they were identified as *T. brevicompactum* described by Degenkolb et al. (2008), and Kraus et al. (2004). Isolates HZA1, HZA2 and HZA13 grown on CMD had similarly morphological characteristics. Conidiophores typically unilateral although paired branches. Phialides straight or sinuous, wide at the base, typically flask-shaped and enlarged in the middle, constricted to the tip. Conidia, 2.5–3.5 × 2.4–3.2 µm, subglobose to ovoidal. They were identified as *T. atroviride*, being identical with description by Dodd et al. (2003). Similarly, based on morphological characteristics, isolate HZA3 was identified as *T. afroharzianum* (Chaverri et al., 2015), HZA6 as *T. koningiopsis* (Samuels et al., 2006), HZA9 as *T. citrinoviride* (Bissett, 1984), HZA10 as *T. asperellum* (Samuels et al., 1999), HZA11 as *T. harzianum* (Samuels et al., 2002), and HZA14 as *T. virens* (Chaverri et al., 2001).

3.4. Inhibitory activity of culture liquid against P. capsici

The inhibitory activity of 15 isolates metabolites against the hyphae growth of *P. capsici* was assessed. All metabolites from different isolates indicated different levels of inhibitory activity ($p < 0.05$) (Table 1). The metabolites produced by *T. virens* HZA14 completely inhibited the hyphae growth after diluted 20 or 40-folds, showing the highest inhibition percentage (100%), followed by *T. afroharzianum* HZA3 with 44.85% (20-folds) and 78.96% (40-folds) inhibition and *T. citrinoviride* HZA9 with 42.445% (20-folds) and 77.81% (40-folds) as well as *T. dorothopsis* HZA5, HZA8 and HZA15 with 34.67–39.59% (20-folds) and 71.0–771.33% (40-folds) and *T. koningiopsis* HZA6 with 37.29% (20-folds) and 72.18% (40-folds). While the lowest inhibition percentage was found in *T. atroviride* HZA1, HZA2 and HZA13, *T. asperellum* HZA10 and *T. harzianum* HZA11 with 0.62–1.59% (20-folds) and 5.18%- 6.29% inhibition.

3.5. Purification and identification of active metabolites

Based on the results of inhibitory activity, potentially active compounds produced by *T. virens* HZA14 were extracted and separated to give four fractions (A, B, C and D). Different amounts of factions A, B, C and D were recovered. The activity tests showed that only fraction C dissolved in DMSO had the strong inhibitory activity against hypha growth of *P. capsici*.

The fraction C was purified with a HPLC instrument, and analyzed by the mass spectrometer. Fullscan MS showed a ion at *m/z* 349 corresponding to the sodium adduct of gliotoxin $[M + Na]^+$ (Fig. 6), which produced its single major daughter ion at *m/z* 263 corresponding

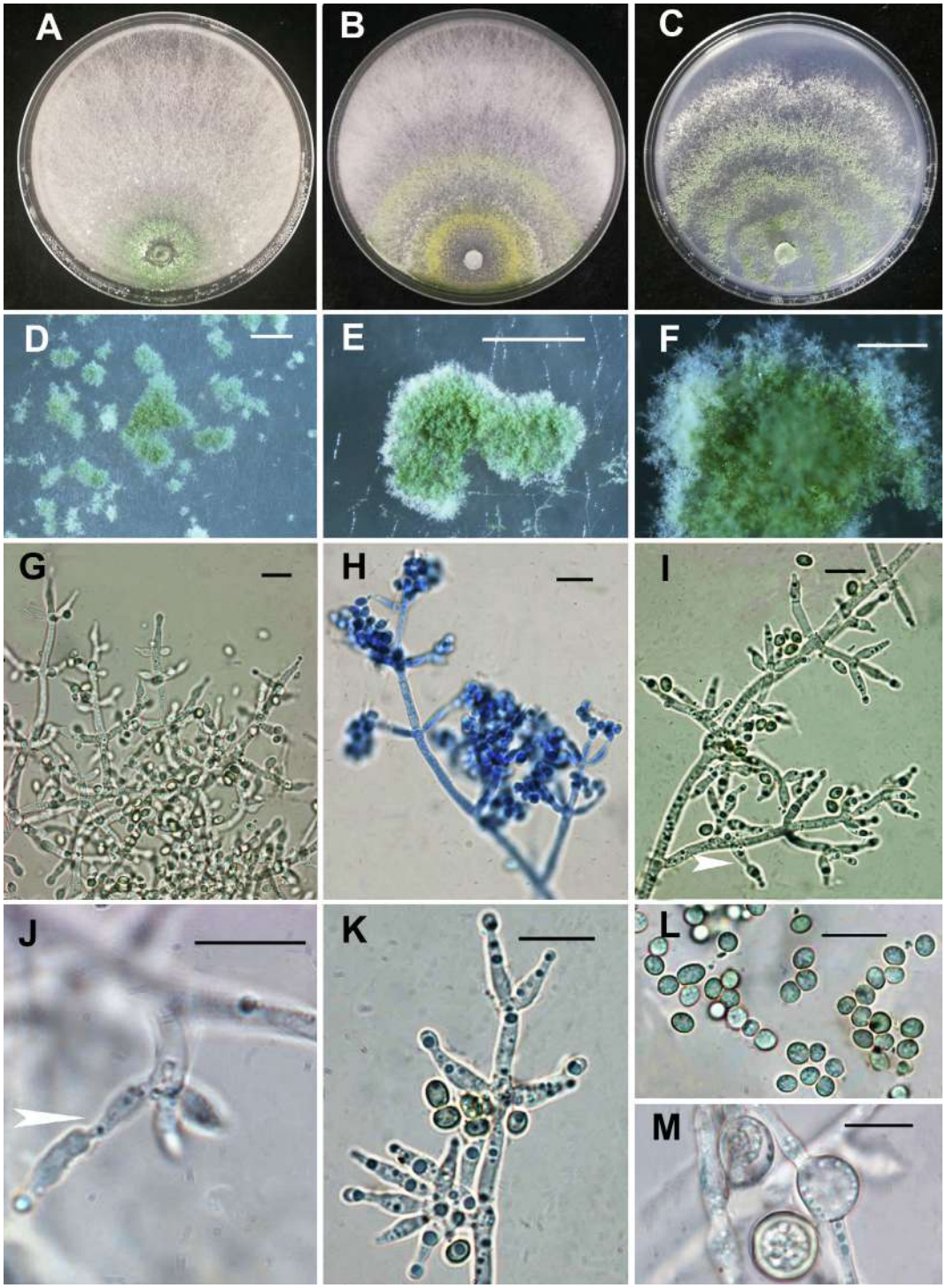

Fig. 5. *Trichoderma dorothopsis* grown on PDA or CMD or SNA in 9-cm-diam Petri dishes under 12 h darkness /12 h light for four days. A. On PDA. B. On CMD. C. On SNA. D-M. On CMD. D-F. Conidial pustules. Individual plumose conidiophores can be seen in the pustule (F). G-K. Conidiophores and phialides. The percurrently proliferated phialides can be seen in (I and J) (arrows). L. Conidia. M. Chlamydospores. Scale bars: D and E = 1 mm; F = 500 μm; G–M = 10 μm.

to the dethiogliotoxin $[M\text{-}2S]^+$, as reported in previous MS studies of gliotoxin by electronic impact mass spectrometry (Bose et al., 1968; Grovel et al., 2002). The isotopic distribution of this daughter ion confirmed a lack of two sulphur atoms in its composition (Bose et al., 1968). The ions at *m/z* 245 correlated to $[M-2S-H_2O]^+$ (Grovel et al., 2002), being attributable to a fragmentation of the daughter ions of the *m/z* 285 ion (Svahn et al., 2012).

Subsequently, the activity test using purified gliotoxin was conducted on the plates containing V8 media (Fig. 7). The activity tests showed that 0.5 μg/ml of gliotoxin inhibited in 40% mycelial growth after incubation for 4 d, 1.0 μg/ml in 66%., while 5.0 μg/ml and more completely inhibited the pathogen growth.

3.6. Inhibitory efficacy against chili pepper blight

Inoculation tests showed that the *T. virens* HZA14 was able to delay disease occurrence and significantly reduced the disease incidence and severity. Five days after inoculation, dark brown lesions were observed

Table 1
Inhibitory activity of metabolites produced from 15 Trichoderma isolates against hyphae growth of *P. capsici*.

Isolates	[a] Inhibition Percentage (%)	
	[b] 40-folds	20-folds
HZA1	1.11 ± 0.62[e]	6.29 ± 0.05[e]
HZA2	1.11 ± 0.62[e]	6.18 ± 0.02[e]
HZA3	44.85 ± 0.44[b]	78.96 ± 1.05[b]
HZA4	15.93 ± 0.77[d]	23.74 ± 0.74[d]
HZA5	34.67 ± 0.21[c]	71.07 ± 0.64[c]
HZA6	37.29 ± 0.50[c]	72.18 ± 0.92[c]
HZA7	13.51 ± 0.56[d]	21.17 ± 0.28[d]
HZA8	34.97 ± 0.60[c]	70.92 ± 0.19[c]
HZA9	42.44 ± 0.20[b]	77.81 ± 0.72[b]
HZA10	0.62 ± 0.05[e]	5.92 ± 0.11[e]
HZA11	1.59 ± 0.04[e]	07.40 ± 0.16[e]
HZA12	16.52 ± 0.22[d]	20.70 ± 0.15[d]
HZA13	1.11 ± 0.12[e]	5.18 ± 0.03[e]
HZA14	100.00 ± 0.00[a]	100.00 ± 0.00[a]
HZA15	39.59 ± 0.57[c]	71.33 ± 0.54[c]

[a] Inhibition percentage (%) of diameter growth of *P. capsici* hyphae on PDA containing the diluted culture liquid five days after inoculation.

[b] The culture liquid was diluted 40-folds or 20-folds. Means in the columns followed by the different letters are significantly different at $p < 0.05$ according to LSD.

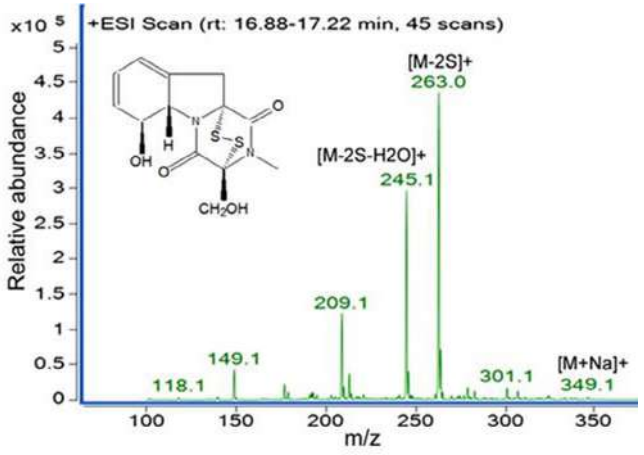

Fig. 6. Fullscan mass spectrum of fraction C. MS spectrum of fraction C showing loss of the two sulphur atoms leading to dethiogliotoxin at *m/z* 263.

on stem bases of few seedlings treated only with the zoospores suspension of *P. capsici* (control). Ten days after inoculation, symptoms of leaf wilting were observed in control plants but no symptom was found in plants coinnoculated with the HZA14 isolate and zoospores suspension. However, typical symptoms appeared on stem bases of plants coinoculated with the HZA14 and zoospores suspension 12 days after inoculation. Fourteen days after inoculation, the lesion extension was obvious on stem bases of plants coinoculated with the HZA14 and zoospores suspension (Fig. 8A). During this period, wilt and damping-off occurred seriously on control plants (Fig. 8B). Fifteen days after inoculation, the disease incidence and disease severity on plants coinoculated with HZA14 and zoospores suspension were 29.84 ± 2.6% and 14.18 ± 0.6%, respectively, compared with control with 92.48 ± 2.1% DI and 88.38 ± 2.9% DS, respectively (Fig. 8C). The HZA14 significantly decreased the disease incidence (62.64%) and severity (64.2%), respectively.

4. Discussion

Trichoderma species have a cosmopolitan distribution and inhabit diverse ecological niches, frequently finding on dead wood and bark, on other fungi, in soil and living within healthy plant roots, stems and leaves (Du Plessis et al., 2018; Mukherjee et al., 2013). In recent years, the number of *Trichoderma* species has dramatically increased. Until now, more than 290 *Trichoderma* species have been described (Bissett et al., 2015; Du Plessis et al., 2018; Zhu et al., 2017). In this study, a new species *T. dorothopsis* from soil was found. However, the *Trichoderma* species still will probably increase because fungal soil communities from many parts of the country have not yet been investigated widely.

In phylogenetic analysis, *T. dorothopsis* has a closest phylogenetic relationship with *T. koningiopsis* to form a well-supported branch that separated it from its relatives, while in morphology, it can be distinguished clearly from *T. koningiopsis* by globose conidia and percurrently proliferated phialides. The molecular and morphological analysis all confirms that *T. dorothopsis* is an unreported new species. However, we also found that several species had a larger base variation range in their gene sequences. In the isolate HZA4, HZA7, and HZA12, phylogenetic analysis displayed that they clustered as a clade, which formed a sister clade with *T. brevicompactum* TRS859 (Fig. 4). Although they had more than 20-base difference comparing with the isolate TRS859 only in *TEF1* gene sequences, morphological data did not support to separate them from *T. brevicompactum* as a distinct species, showing that *T. brevicompactum* had a larger variation range in its gene sequences. Similarly, five reference isolates and test isolates (HZA1, HZA2 and HZA13) in *T. atroviride* indicated a larger base variation rang in tree-loci sequences as well. So our study provides another demarcation information about *Trichoderma* species.

Several species of *Trichoderma* have been shown to be particularly effective in controlling pepper blight (Ezziyyani et al., 2007; Osorio-Hernández et al., 2011; Sid Ahmed et al., 1999). Our results showed that 19.5% of *Trichoderma* species isolates had high antagonistic activities against the mycelial growth of *P. capsici*, especially *T. virens* HZA14 caused a distinct interaction zone of hyphal disappearance of *P. capsici* HZ07 (Fig. 2). This was considered to be related to its metabolites. A few studies have showed that in interaction between mycoparasites and plant pathogens, interaction zone of hyphal disappearance are not observed (Cao et al., 2009), as showed in Fig. 1A-M and O in this study. Although *T. virens* HZA14 possesses mycoparasitism, as showed in Fig. 3B and 3C, rapid colony disintegration is distinctly related to another mechanism. Microscopic observations demonstrated that a partially killed hypha of *P. capsici* could be related to antagonistic compounds produced by *T. virens* in the interaction zone of *P. capsici* hyphal disappearance (Fig. 3A). Therefore, antagonistic compounds produced by *T. virens* HZA14 may play an important role in antagonistic mechanisms. Subsequently, *in vitro* test confirmed that its culture liquid had high inhibitory activity (Table 1). Chemical structure of an active fraction obtained from the culture liquid was identified as gliotoxin. Production of gliotoxin by *T. viride* has been known since it was discovered by Brian (1944). Gliotoxin displays a wide range of biological effects including anti-viral, anti-bacterial and immunosuppressive properties (Niide et al., 2006; Prakesh Hebbar and Lumsden, 1999). Production of gliotoxin by *T. virens* has been proposed as an important component in antibiosis (Fravel, 2003). Gliotoxin has also been reported to act synergistically with chitinase in the antifungal activities of *T. virens* (Dipietro et al., 1993). Similarly, the isolates producing gliotoxin were more effective in seed treatments for controlling diseases caused by *Rhizoctonia solani* (Howell et al., 1993). These studies showed that gliotoxin may play an important role in reducing pathogen development and disease occurrence, while this study charactered relationship of gliotoxin with formation of interaction zone of pathogen hyphal disappearance for first time and revealed its anti-oomycetes activity. Bioactivity of gliotoxin produced by the HZA14 against hyphal growth of *P. capsici* was very high in *in vitro* tests on PDA. *In vivo* inoculation tests showed that the HZA14 isolate was able to delay disease occurrence and significantly reduce disease incidence and

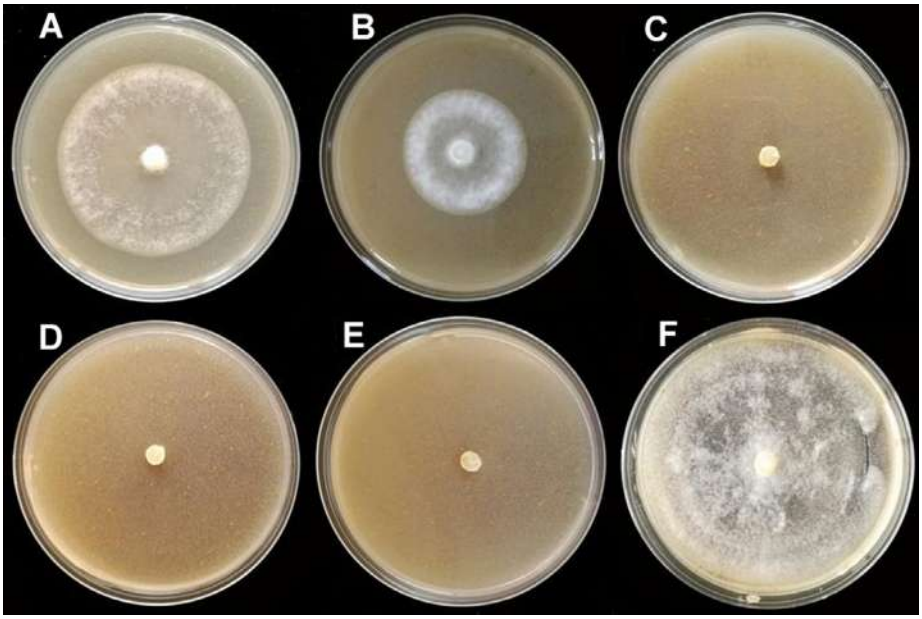

Fig. 7. The gliotoxin activity against hyphal growth of *P. capsici* on PDA plates with different concentrations of gliotoxin. A. With 0.5 μg ml^{-1} of gliotoxin. B. With 1.0 μg ml^{-1} of gliotoxin. C. With 5.0 μg ml^{-1} of gliotoxin. D. With 10.0 μg ml^{-1} of gliotoxin. E. With 15.0 μg ml^{-1} of gliotoxin. F. Control.

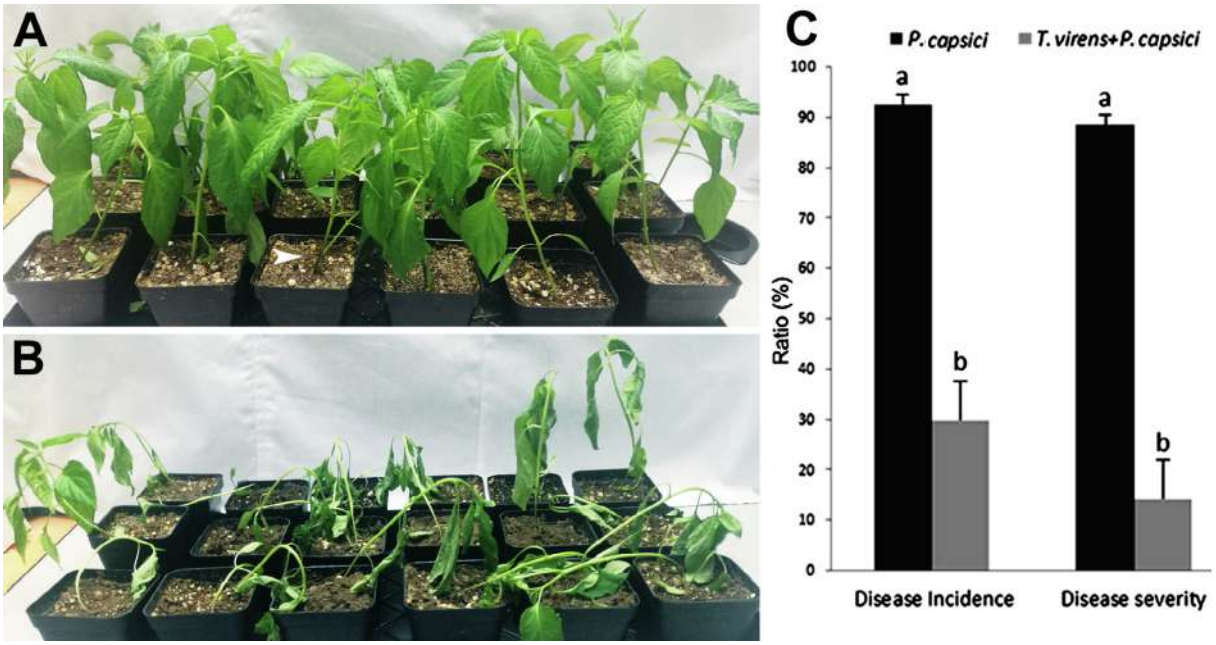

Fig. 8. Effect of inoculation with *T. virens* HZA14 on the disease incidence and severity of chili pepper blight 14 days after inoculation. A–B. Disease symptoms 14 days after inoculation. A. Coinoculation with isolate HZA14 and zoospores suspension of *P. capsici*. The lesions spread upward (arrow). B. Inoculation with zoospores suspension (control). C. Disease incidence and severity 15 days after inoculation. Vertical bars represent standard deviation of the means (n = 3). Bars followed by the different letters are significantly different at $p < 0.05$ according to LSD.

severity by 62.64% and 64.20%, respectively. However, inhibitory role of the HZA14 against pathogen also involves in other mechanisms of action.

A great number of studies showed that *Trichoderma* spp. possess the multiple mechanisms, including mycoparasitism, extracellular enzymes such as cellulase, amylase, pectinase, protease and chitinase, antagonistic compounds and induced resistance, to inhibit pathogens and reduce diseases (Atanasova et al., 2013; Cherkupally et al., 2017; Vargas et al., 2014). As showing in Fig. 1, the antagonistic *Trichoderma* spp. isolates colonized and degraded the colony growth of pathogen by means of penetration and encirclement (Fig. 2C and 2D), obviously being associated with the mechanism of mycoparasitism involving in production of extracellularly lytic enzymes. Thus the *Trichoderma* HZA14 possibly uses multiple mechanisms of action to synergistically inhibit pathogen, while gliotoxin produced by it could play an important role in inhibiting pathogen and controlling chili pepper blight.

Our data indicate that the *Trichoderma* HZA14 and the gliotoxins that it produces have a great potential using as candidate biocontrol agent. However, its biocontrol efficacy needs to be confirmed under the field condition for generating useful products for management of pathogens in the agroecosystem. Therefore, further studies will focus on its control efficacy in the fields for development of biocontrol agent.

Acknowledgements

This work was supported by the Key Science and Technology Project of Zhejiang Province (No. 2015C02023), Special Fund for Agro-scientific Research in the Public Interest of China (No. 201503109) and National Natural Science Foundation of China (31501342).

Appendix A. Supplementary data

Supplementary data to this article can be found online at https://doi.org/10.1016/j.biocontrol.2020.104261.

References

Atanasova, L., Le Crom, S., Gruber, S., Coulpier, F., Seidl-Seiboth, V., Kubicek, C., Druzhinina, I., 2013. Comparative transcriptomics reveals different strategies of *Trichoderma mycoparasitism*. BMC Genomics 14, 121–135.

Barchenger, D.W., Lamour, K.H., Bosland, P.W., 2018. Challenges and strategies for breeding resistance in *Capsicum annuum* to the multifarious pathogen *Phytophthora capsici*. Front. Plant. Sci. 9, 628.

Bissett, J., 1984. A revision of the genus *Trichoderma*. I. section Longibrachiatum sect. nov. Can. J. Bot. 62, 924–931.

Bissett, J., 1991. A revision of the genus *Trichoderma*. III. section *Pachybasium*. Can. J. Bot. 69, 2373–2417.

Bissett, J., Gams, W., Jaklitsch, W., Samuels, G.J., 2015. Accepted *Trichoderma* names in the year 2015. IMA fungus 6, 263–295.

Bose, A.K., Das, K.G., Funke, P.T., Kugajevsky, I., Shukla, O.P., Khanchandani, K.S., Suhadolnik, R.J., 1968. Biosynthetic studies on gliotoxin using stable isotopes and mass spectral methods. J. Am. Chem. Soc. 90, 1038–1041.

Bosland, P., Lindsey, D., 1991. A seedling screen for *Phytophthora* root rot of pepper *Capsicum annuum*. Plant Dis. 75, 1048–1050.

Brian, P.W., 1944. Production of gliotoxin by *Trichoderma viride*. Nature 154, 667–668.

Callaghan, S.E., Williams, A.P., Burgess, T., White, D., Keovorlajak, T., Phitsanoukane, P., Phantavong, S., Vilavong, S., Ireland, K.B., Duckitt, G.S., Burgess, L.W., 2016. First report of *Phytophthora capsici* in the Lao PDR. Australasian Plant Dis. Notes 11, 22.

Cao, R., Liu, X., Gao, K., Mendgen, K., Kang, Z., Gao, J., Dai, Y., Wang, X., 2009. Mycoparasitism of endophytic fungi isolated from reed on soilborne phytopathogenic fungi and production of cell wall-degrading enzymes in vitro. Curr. Microbiol. 59, 584–592.

Carbone, I., Kohn, L.M., 1999. A method for designing primer sets for speciation studies in filamentous ascomycetes. Mycologia 91, 553–556.

Chaverri, P., Branco-Rocha, F., Jaklitsch, W., Gazis, R., Degenkolb, T., Samuels, G.J., 2015. Systematics of the *Trichoderma harzianum* species complex and the re-identification of commercial biocontrol strains. Mycologia 107, 558–590.

Chaverri, P., Samuels, G.J., Stewart, E.L., 2001. *Hypocrea virens* sp. nov., the teleomorph of *Trichoderma virens*. Mycologia 93, 1113–1124.

Cherkupally, R., Amballa, H., Reddy Bhoomi, N., 2017. *In vitro* screening for enzymatic activity of *Trichoderma* species for biocontrol potential. Ann. Plan. Sci. 6, 1784–1789.

Darriba, D., Taboada, G.L., Doallo, R., Posada, D., 2012. jModelTest 2: more models, new heuristics and parallel computing. Nat. Methods 9, 772.

Degenkolb, T., Dieckmann, R., Nielsen, K., Gräfenhan, T., Theis, C., Zafari, D., Chaverri, P., Ismaiel, A., Brueckner, H., Döhren, H., Thrane, U., Petrini, O., J Samuels, G., 2008. The *Trichoderma brevicompactum* clade: A separate lineage with new species, new peptabiotics, and mycotoxins. Mycol. Prog. 7, 177–219.

Dennis, C., Webster, J., 1971. Antagonistic properties of species-groups of *Trichoderma*: II. production of volatile antibiotics. Trans. Br. Mycol. Soc. 57, 25–39.

Dipietro, A., Lorito, M., Hayes, C.K., Broadway, R.M., Harman, G.E., 1993. Endochitinase from *Gliocladium virens*: isolation, characterization, and synergistic antifungal activity in combination with gliotoxin. Phytopathology 83, 308–313.

Dodd, S.L., Lieckfeldt, E., Samuels, G.J., 2003. *Hypocrea atroviridis* sp. nov., the teleomorph of *Trichoderma atroviride*. Mycologia 95, 27–40.

Du Plessis, I.L., Druzhinina, I.S., Atanasova, L., Yarden, O., Jacobs, K., 2018. The diversity of *Trichoderma* species from soil in south Africa, with five new additions. Mycologia 110, 559–583.

Dunn, A.R., Smart, C.D., 2015. Interactions of *Phytophthora capsici* with resistant and susceptible pepper roots and stems. Phytopathology 105, 1355–1361.

El-Hasan, A., Walker, F., Schöne, J., Buchenauer, H., 2009. Detection of viridiofungin A and other antifungal metabolites excreted by *Trichoderma harzianum* active against different plant pathogens. Eur. J. of Plant Pathol. 124, 457–470.

Elad, Y., Chet, I., Henis, Y., 1981. A selective medium for improving quantitative isolation of *Trichoderma* spp. from soil. Phytoparasitica 9, 59–67.

Ezziyyani, M., Requena, M.E., Egea-Gilabert, C., Candela, M.E., 2007. Biological control of *Phytophthora* root rot of pepper using *Trichoderma harzianum* and *Streptomyces rochei* in combination. J. Phytopathology 155, 342–349.

Foster, J.M., Hausbeck, M.K., 2010. Resistance of pepper to Phytophthora crown, root, and fruit rot is affected by isolate virulence. Plant Dis. 94, 24–30.

Fravel, R.D., 2003. Role of antibiosis in the biocontrol of plant diseases. Ann. Rev. Phytopathol. 26, 75–91.

Granke, L.L., Quesada-Ocampo, L.M., Lamour, K., Hausbeck, M.K., 2015. Advances in research on Phytophthora capsici on vegetable crops in the united states. Plant Dis. 95, 1588–1600.

Grovel, O., Pouchus, Y.F., Robiou du Pont, T., Montagu, M., Amzil, Z., Verbist, J.F., 2002. Ion trap MS^n for identification of gliotoxin as the cytotoxic factor of a marine strain of *Aspergillus fumigatus* Fresenius. J. Microbiol. Meth. 48, 171–179.

Hall, T., 1999. BioEdit: A user-friendly biological sequence alignment editor and analysis program for windows 95/98/NT. Nucl. Acids Symp. Se. 41, 95–98.

Harman, G.E., 2006. Overview of mechanisms and uses of *Trichoderma* spp. Phytopathology 96, 190–194.

Hausbeck, M.K., Lamour, K.H., 2004. *Phytophthora capsici* on vegetable crops: research progress and management challenges. Plant Dis. 88, 1292–1303.

Howell, C.R., Stipanovic, R.D., Lumsden, R.D., 1993. Antibiotic production by strains of *Gliocladium virens* and its relation to the biocontrol of cotton seedling diseases. Biocon. Sci. Technol. 3, 435–441.

Hyakumachi, M., Nishimura, M., Arakawa, T., Asano, S., Yoshida, S., Tsushima, S., Takahashi, H., 2013. *Bacillus thuringiensis* suppresses bacterial wilt disease caused by *Ralstonia solanacearum* with systemic induction of defense-related gene expression in tomato. Microbes Environ. 28, 128–134.

Jaklitsch, W.M., 2009. European species of *Hypocrea* part I. the green-spored species. Stud. Mycol. 63, 1–91.

Jeleń, H., Błaszczyk, L., Chełkowski, J., Rogowicz, K., Strakowska, J., 2014. Formation of 6-n-pentyl-2H-pyran-2-one (6-PAP) and other volatiles by different *Trichoderma* species. Mycol. Progress 13, 589–600.

Jiang, H., Zhang, L., Zhang, J.-Z., Ojaghian, M.R., Hyde, K.D., 2016a. Antagonistic interaction between *Trichoderma asperellum* and *Phytophthora capsici* in vitro. J Zhejiang Univ Sci B 17, 271–281.

Jiang, Y., Wang, J.-L., Chen, J., Mao, L.-J., Feng, X.-X., Zhang, C.-L., Lin, F.-C., 2016b. *Trichoderma* biodiversity of agricultural fields in east China reveals a gradient distribution of species. PLoS ONE 11, e0160613.

Katoh, K., Standley, D.M., 2013. MAFFT multiple sequence alignment software version 7: improvements in performance and usability. Mol. Biol. Evol. 30, 772–780.

Kraus, G.F., Druzhinina, I., Gams, W., Bissett, J., Zafari, D., Szakacs, G., Koptchinski, A., Prillinger, H., Zare, R., Kubicek, C.P., 2004. *Trichoderma brevicompactum* sp. nov. Mycologia 96, 1059–1073.

Mukherjee, M., Mukherjee, P.K., Horwitz, B.A., Zachow, C., Berg, G., Zeilinger, S., 2012. Trichoderma-plant-pathogen interactions: advances in genetics of biological control. Indian J. Microbiol. 52, 522–529.

Mukherjee, P.K., Horwitz, B.A., Singh, U.S., Mukherjee, M., Schmoll, M., 2013. Trichoderma: Biology and Applications CAB,344, p.

Niide, O., Suzuki, Y., Yoshimaru, T., Inoue, T., Takayama, T., Ra, C., 2006. Fungal metabolite gliotoxin blocks mast cell activation by a calcium- and superoxide-dependent mechanism: implications for immunosuppressive activities. Clin. Immunol. 118, 108–116.

Osorio-Hernández, E., Hernández, D., Morales, G., Rodriguez, R., Castillo, F., 2011. *In vitro* behavior of *Trichoderma* spp. against *Phytophthora capsici* Leonian. Afr. J. Agric. Res. 6, 4594–4600.

Parra, G., Ristaino, J.B., 2001. Resistance to mefenoxam and metalaxyl among field isolates of *Phytophthora capsici* causing Phytophthora blight of bell pepper. Plant Dis. 85, 1069–1075.

Prakesh Hebbar, K., Lumsden, R.D., 1999. Biological control of seedling diseases. In: Hall, F.R., Menn, J.J. (Eds.), Biopesticides: Use and Delivery. Humana Press, Totowa, NJ, pp. 103–116.

Quesada-Ocampo, L.M., Fulbright, D.W., Hausbeck, M.K., 2009. Susceptibility of fraser fir to *Phytophthora capsici*. Plant Dis. 93, 135–141.

Ramírez-Delgado, E., Luna-Ruíz, J.d.J., Moreno-Rico, O., Quiroz-Velásquez, J., Hernández-Mendoza, J.L., 2018. Effect of *Trichoderma* on growth and sporangia production of *Phytophthora capsici*. J. Agric. Sci. 10, 8–15.

Ristaino, J., 1990. Intraspecific variation among isolates of *Phytophthora capsici* from pepper and cucurbit fields in north Carolina. Phytopathology 80, 1253–1259.

Roberts, D.P., Lumsden, R.D., 1990. Effect of extracellular metabolites from *Gliocladium virens* on germination of sporangia and mycelial growth of *Pythium ultimum*. Phytopathology 80, 461–465.

Roberts, P., McGovern, R., A. Kucharek, T., J. Mitchell, D., 2008. Vegetable diseases caused by Phytophthora capsici in Florida SP159,1-6.

Ronquist, F., Teslenko, M., van der Mark, P., Ayres, D.L., Darling, A., Hohna, S., Larget, B., Liu, L., Suchard, M.A., Huelsenbeck, J.P., 2012. MrBayes 3.2: efficient Bayesian phylogenetic inference and model choice across a large model space. Syst. Biol. 61, 539–542.

Samuels, G.J., Dodd, S.L., Lu, B.-S., Petrini, O., Schroers, H.-J., Druzhinina, I.S., 2006. The *Trichoderma koningii* aggregate species. Stud. Mycol. 56, 67–133.

Samuels, G.J., Lieckfeldt, E., Nirenberg, H.I., 1999. *Trichoderma asperellum*, a new species with waited conidia, and redescription of *T. viride*. Sydowia 51, 71–88.

Samuels, J.G., Dodd, S., Gams, W., Castlebury, L., Petrini, O., 2002. *Trichoderma* species associated with the green mold epidemic of commercially grown *Agaricus bisporus*. Mycologia 94, 146–170.

Savazzini, F., Longa, C.M.O., Pertot, I., 2009. Impact of the biocontrol agent *Trichoderma atroviride* SC1 on soil microbial communities of a vineyard in northern Italy. Soil Biol. Biochem. 41, 1457–1465.

Sid Ahmed, A., Pérez-Sánchez, C., Egea, C., Candela, M.E., 1999. Evaluation of *Trichoderma harzianum* for controlling root rot caused by *Phytophthora capsici* in pepper plants. Plant. Pathol. 48, 58–65.

Silvestro, D., Michalak, I., 2012. raxmlGUI: a graphical front-end for RAxML. Org. Divers. Evol. 12, 335–337.

Svahn, K.S., Göransson, U., El-Seedi, H., Bohlin, L., Larsson, D.G.J., Olsen, B., Chryssanthou, E., 2012. Antimicrobial activity of filamentous fungi isolated from highly antibiotic-contaminated river sediment. Infect. Ecol. Epidemiol. 2, 1–6.

Vargas, W.A., Mukherjee, P.K., Laughlin, D., Wiest, A., Moran-Diez, M.E., Kenerley, C.M., 2014. Role of gliotoxin in the symbiotic and pathogenic interactions of *Trichoderma*

virens. Microbiology 160, 2319–2330.
Vinale, F., Sivasithamparam, K., Ghisalberti, E.L., Marra, R., Barbetti, M.J., Li, H., Woo, S.L., Lorito, M., 2008. A novel role for *Trichoderma* secondary metabolites in the interactions with plants. Physiol. Mol. Plant Pathol. 72, 80–86.
Zhang, J.Z., Li, M.J., 2009. A new species of *Bipolaris* from the halophyte *Sesuvium portulacastrum* in guangdong province, China. Mycotaxon 109, 289–300.
Zhang, W., Zhang, L., Sun, Y., 2015. Size-controlled green synthesis of silver nanoparticles assisted by L-cysteine. Front. Chem. Sci. Eng. 9, 494–500.
Zhu, Z.X., Xu, H.X., Zhuang, W.Y., Li, Y., 2017. Two new green-spored species of *Trichoderma* (sordariomycetes, ascomycota) and their phylogenetic positions. MycoKeys 26, 61–75.